

# Collins and Sivers asymmetries for pions and kaons in muon–deuteron DIS

The COMPASS Collaboration

## Abstract

The measurements of the Collins and Sivers asymmetries of identified hadrons produced in deep-inelastic scattering of 160 GeV/ $c$  muons on a transversely polarised  ${}^6\text{LiD}$  target at COMPASS are presented. The results for charged pions and charged and neutral kaons correspond to all data available, which were collected from 2002 to 2004. For all final state particles both, the Collins and Sivers asymmetries turn out to be small, compatible with zero within the statistical errors, in line with the previously published results for not identified charged hadrons, and with the expected cancellation between the u- and d-quark contributions.

Keywords: transversity, deuteron, transverse single-spin asymmetry, identified hadrons, Collins asymmetry, Sivers asymmetry, COMPASS.

PACS 13.60.-r, 13.88.+e, 14.20.Dh, 14.65.-q

*Physics Letters B*

# The COMPASS Collaboration

M. Alekseev<sup>32)</sup>, V.Yu. Alexakhin<sup>8)</sup>, Yu. Alexandrov<sup>18)</sup>, G.D. Alexeev<sup>8)</sup>, A. Amoroso<sup>30)</sup>,  
 A. Arbuzov<sup>8)</sup>, B. Badełek<sup>33)</sup>, F. Balestra<sup>30)</sup>, J. Ball<sup>25)</sup>, J. Barth<sup>4)</sup>, G. Baum<sup>1)</sup>, Y. Bedfer<sup>25)</sup>,  
 C. Bernet<sup>25)</sup>, R. Bertini<sup>30)</sup>, M. Bettinelli<sup>19)</sup>, R. Birsa<sup>27)</sup>, J. Bisplinghoff<sup>3)</sup>, P. Bordalo<sup>15,a)</sup>,  
 F. Bradamante<sup>28)</sup>, A. Bravar<sup>16,27)</sup>, A. Bressan<sup>28,11)</sup>, G. Brona<sup>33)</sup>, E. Burtin<sup>25)</sup>, M.P. Bussa<sup>30)</sup>,  
 A. Chapiro<sup>29)</sup>, M. Chiosso<sup>30)</sup>, A. Cicuttin<sup>29)</sup>, M. Colantoni<sup>31)</sup>, S. Costa<sup>30,+)</sup>, M.L. Crespo<sup>29)</sup>,  
 S. Dalla Torre<sup>27)</sup>, T. Dafni<sup>25)</sup>, S. Das<sup>7)</sup>, S.S. Dasgupta<sup>6)</sup>, R. De Masi<sup>20)</sup>, N. Dedek<sup>19)</sup>,  
 O.Yu. Denisov<sup>31,b)</sup>, L. Dhara<sup>7)</sup>, V. Diaz<sup>29)</sup>, A.M. Dinkelbach<sup>20)</sup>, S.V. Donskov<sup>24)</sup>,  
 V.A. Dorofeev<sup>24)</sup>, N. Doshita<sup>21)</sup>, V. Duic<sup>28)</sup>, W. Dünneweber<sup>19)</sup>, P.D. Eversheim<sup>3)</sup>,  
 A.V. Efremov<sup>8)</sup>, W. Eyrich<sup>9)</sup>, M. Faessler<sup>19)</sup>, V. Falaleev<sup>11)</sup>, A. Ferrero<sup>30,11)</sup>, L. Ferrero<sup>30)</sup>,  
 M. Finger<sup>22)</sup>, M. Finger jr.<sup>8)</sup>, H. Fischer<sup>10)</sup>, C. Franco<sup>15)</sup>, J. Franz<sup>10)</sup>, J.M. Friedrich<sup>20)</sup>,  
 V. Frolov<sup>30,b)</sup>, R. Garfagnini<sup>30)</sup>, F. Gautheron<sup>1)</sup>, O.P. Gavrichtchouk<sup>8)</sup>, R. Gazda<sup>33)</sup>,  
 S. Gerassimov<sup>18,20)</sup>, R. Geyer<sup>19)</sup>, M. Giorgi<sup>28)</sup>, B. Gobbo<sup>27)</sup>, S. Goertz<sup>2,4)</sup>, A.M. Gorin<sup>24)</sup>,  
 S. Grabmüller<sup>20)</sup>, O.A. Grajek<sup>33)</sup>, A. Grasso<sup>30)</sup>, B. Grube<sup>20)</sup>, R. Gushterski<sup>8)</sup>, A. Guskov<sup>8)</sup>,  
 F. Haas<sup>20)</sup>, J. Hannappel<sup>4)</sup>, D. von Harrach<sup>16)</sup>, T. Hasegawa<sup>17)</sup>, J. Heckmann<sup>2)</sup>, S. Hedicke<sup>10)</sup>,  
 F.H. Heinsius<sup>10)</sup>, R. Hermann<sup>16)</sup>, C. Heß<sup>2)</sup>, F. Hinterberger<sup>3)</sup>, M. von Hodenberg<sup>10)</sup>,  
 N. Horikawa<sup>21,c)</sup>, S. Horikawa<sup>21)</sup>, N. d'Hose<sup>25)</sup>, C. Ilgner<sup>19)</sup>, A.I. Ioukaev<sup>8)</sup>, S. Ishimoto<sup>21)</sup>,  
 O. Ivanov<sup>8)</sup>, Yu. Ivanshin<sup>8)</sup>, T. Iwata<sup>21,35)</sup>, R. Jahn<sup>3)</sup>, A. Janata<sup>8)</sup>, P. Jasinski<sup>16)</sup>, R. Joosten<sup>3)</sup>,  
 N.I. Jouravlev<sup>8)</sup>, E. Kabuß<sup>16)</sup>, D. Kang<sup>10)</sup>, B. Ketzer<sup>20)</sup>, G.V. Khaustov<sup>24)</sup>, Yu.A. Khokhlov<sup>24)</sup>,  
 Yu. Kisselev<sup>1,2)</sup>, F. Klein<sup>4)</sup>, K. Klimaszewski<sup>33)</sup>, S. Koblitiz<sup>16)</sup>, J.H. Koivuniemi<sup>13,2)</sup>,  
 V.N. Kolosov<sup>24)</sup>, E.V. Komissarov<sup>8,+)</sup>, K. Kondo<sup>21)</sup>, K. Königsmann<sup>10)</sup>, I. Konorov<sup>18,20)</sup>,  
 V.F. Konstantinov<sup>24)</sup>, A.S. Korentchenko<sup>8)</sup>, A. Korzenev<sup>16,b)</sup>, A.M. Kotzinian<sup>8,30)</sup>,  
 N.A. Koutchinski<sup>8)</sup>, O. Kouznetsov<sup>8,25)</sup>, A. Kral<sup>23)</sup>, N.P. Kravchuk<sup>8)</sup>, Z.V. Kroumchtein<sup>8)</sup>,  
 R. Kuhn<sup>20)</sup>, F. Kunne<sup>25)</sup>, K. Kurek<sup>33)</sup>, M.E. Ladygin<sup>24)</sup>, M. Lamanna<sup>11,28)</sup>, J.M. Le Goff<sup>25)</sup>,  
 A.A. Lednev<sup>24)</sup>, A. Lehmann<sup>9)</sup>, S. Levorato<sup>28)</sup>, J. Lichtenstadt<sup>26)</sup>, T. Liska<sup>23)</sup>, I. Ludwig<sup>10)</sup>,  
 A. Maggiora<sup>31)</sup>, M. Maggiora<sup>30)</sup>, A. Magnon<sup>25)</sup>, G.K. Mallot<sup>11)</sup>, A. Mann<sup>20)</sup>, C. Marchand<sup>25)</sup>,  
 J. Marroncle<sup>25)</sup>, A. Martin<sup>28)</sup>, J. Marzec<sup>34)</sup>, F. Massmann<sup>3)</sup>, T. Matsuda<sup>17)</sup>,  
 A.N. Maximov<sup>8,+)</sup>, W. Meyer<sup>2)</sup>, A. Mielech<sup>27,33)</sup>, Yu.V. Mikhailov<sup>24)</sup>, M.A. Moinester<sup>26)</sup>,  
 A. Mutter<sup>10,16)</sup>, A. Nagaytsev<sup>8)</sup>, T. Nagel<sup>20)</sup>, O. Nähle<sup>3)</sup>, J. Nassalski<sup>33)</sup>, S. Neliba<sup>23)</sup>,  
 F. Nerling<sup>10)</sup>, S. Neubert<sup>20)</sup>, D.P. Neyret<sup>25)</sup>, V.I. Nikolaenko<sup>24)</sup>, K. Nikolaev<sup>8)</sup>,  
 A.G. Olshevsky<sup>8)</sup>, M. Ostrick<sup>4)</sup>, A. Padee<sup>34)</sup>, P. Pagano<sup>28)</sup>, S. Panebianco<sup>25)</sup>, R. Panknin<sup>4)</sup>,  
 D. Panziera<sup>32)</sup>, S. Paul<sup>20)</sup>, B. Pawlukiewicz-Kaminska<sup>33)</sup>, D.V. Peshekhonov<sup>8)</sup>,  
 V.D. Peshekhonov<sup>8)</sup>, G. Piragino<sup>30)</sup>, S. Platchkov<sup>25)</sup>, J. Pochodzalla<sup>16)</sup>, J. Polak<sup>14)</sup>,  
 V.A. Polyakov<sup>24)</sup>, J. Pretz<sup>4)</sup>, S. Procureur<sup>25)</sup>, C. Quintans<sup>15)</sup>, J.-F. Rajotte<sup>19)</sup>, S. Ramos<sup>15,a)</sup>,  
 V. Rapatsky<sup>8)</sup>, G. Reicherz<sup>2)</sup>, D. Reggiani<sup>11)</sup>, A. Richter<sup>9)</sup>, F. Robinet<sup>25)</sup>, E. Rocco<sup>27,30)</sup>,  
 E. Rondio<sup>33)</sup>, A.M. Rozhdestvensky<sup>8)</sup>, D.I. Ryabchikov<sup>24)</sup>, V.D. Samoylenko<sup>24)</sup>, A. Sandacz<sup>33)</sup>,  
 H. Santos<sup>15,a)</sup>, M.G. Sapozhnikov<sup>8)</sup>, S. Sarkar<sup>7)</sup>, I.A. Savin<sup>8)</sup>, P. Schiavon<sup>28)</sup>, C. Schill<sup>10)</sup>,  
 L. Schmitt<sup>20,d)</sup>, P. Schönmeier<sup>9)</sup>, W. Schröder<sup>9)</sup>, O.Yu. Shevchenko<sup>8)</sup>, H.-W. Siebert<sup>12,16)</sup>,  
 L. Silva<sup>15)</sup>, L. Sinha<sup>7)</sup>, A.N. Sissakian<sup>8)</sup>, M. Slunecka<sup>8)</sup>, G.I. Smirnov<sup>8)</sup>, S. Sosio<sup>30)</sup>, F. Sozzi<sup>28)</sup>,  
 A. Srnka<sup>5)</sup>, F. Stinzing<sup>9)</sup>, M. Stolarski<sup>33,10)</sup>, V.P. Sugonyaev<sup>24)</sup>, M. Sulc<sup>14)</sup>, R. Sulej<sup>34)</sup>,  
 V.V. Tchalishvili<sup>8)</sup>, S. Tessaro<sup>27)</sup>, F. Tessarotto<sup>27)</sup>, A. Teufel<sup>9)</sup>, L.G. Tkatchev<sup>8)</sup>,  
 G. Venugopal<sup>3)</sup>, M. Virius<sup>23)</sup>, N.V. Vlassov<sup>8)</sup>, A. Vossen<sup>10)</sup>, R. Webb<sup>9)</sup>, E. Weise<sup>3,10)</sup>,  
 Q. Weitzel<sup>20)</sup>, R. Windmolders<sup>4)</sup>, S. Wirth<sup>9)</sup>, W. Wiślicki<sup>33)</sup>, H. Wollny<sup>10)</sup>, K. Zaremba<sup>34)</sup>,  
 M. Zavertyaev<sup>18)</sup>, E. Zemlyanichkina<sup>8)</sup>, J. Zhao<sup>16,27)</sup>, R. Ziegler<sup>3)</sup> and A. Zvyagin<sup>19)</sup>

- 
- 1) Universität Bielefeld, Fakultät für Physik, 33501 Bielefeld, Germany<sup>e)</sup>
  - 2) Universität Bochum, Institut für Experimentalphysik, 44780 Bochum, Germany<sup>e)</sup>
  - 3) Universität Bonn, Helmholtz-Institut für Strahlen- und Kernphysik, 53115 Bonn, Germany<sup>e)</sup>
  - 4) Universität Bonn, Physikalisches Institut, 53115 Bonn, Germany<sup>e)</sup>
  - 5) Institute of Scientific Instruments, AS CR, 61264 Brno, Czech Republic<sup>f)</sup>
  - 6) Burdwan University, Burdwan 713104, India<sup>g)</sup>
  - 7) Matrivani Institute of Experimental Research & Education, Calcutta-700 030, India<sup>h)</sup>
  - 8) Joint Institute for Nuclear Research, 141980 Dubna, Moscow region, Russia
  - 9) Universität Erlangen–Nürnberg, Physikalisches Institut, 91054 Erlangen, Germany<sup>e)</sup>
  - 10) Universität Freiburg, Physikalisches Institut, 79104 Freiburg, Germany<sup>e)</sup>
  - 11) CERN, 1211 Geneva 23, Switzerland
  - 12) Universität Heidelberg, Physikalisches Institut, 69120 Heidelberg, Germany<sup>e)</sup>
  - 13) Helsinki University of Technology, Low Temperature Laboratory, 02015 HUT, Finland and University of Helsinki, Helsinki Institute of Physics, 00014 Helsinki, Finland
  - 14) Technical University in Liberec, 46117 Liberec, Czech Republic<sup>f)</sup>
  - 15) LIP, 1000-149 Lisbon, Portugal<sup>i)</sup>
  - 16) Universität Mainz, Institut für Kernphysik, 55099 Mainz, Germany<sup>e)</sup>
  - 17) University of Miyazaki, Miyazaki 889-2192, Japan<sup>j)</sup>
  - 18) Lebedev Physical Institute, 119991 Moscow, Russia
  - 19) Ludwig-Maximilians-Universität München, Department für Physik, 80799 Munich, Germany<sup>e,k)</sup>
  - 20) Technische Universität München, Physik Department, 85748 Garching, Germany<sup>e,k)</sup>
  - 21) Nagoya University, 464 Nagoya, Japan<sup>j)</sup>
  - 22) Charles University, Faculty of Mathematics and Physics, 18000 Prague, Czech Republic<sup>f)</sup>
  - 23) Czech Technical University in Prague, 16636 Prague, Czech Republic<sup>f)</sup>
  - 24) State Research Center of the Russian Federation, Institute for High Energy Physics, 142281 Protvino, Russia
  - 25) CEA DAPNIA/SPhN Saclay, 91191 Gif-sur-Yvette, France
  - 26) Tel Aviv University, School of Physics and Astronomy, 69978 Tel Aviv, Israel<sup>l)</sup>
  - 27) Trieste Section of INFN, 34127 Trieste, Italy
  - 28) University of Trieste, Department of Physics and Trieste Section of INFN, 34127 Trieste, Italy
  - 29) Abdus Salam ICTP and Trieste Section of INFN, 34127 Trieste, Italy
  - 30) University of Turin, Department of Physics and Torino Section of INFN, 10125 Turin, Italy
  - 31) Torino Section of INFN, 10125 Turin, Italy
  - 32) University of Eastern Piedmont, 1500 Alessandria, and Torino Section of INFN, 10125 Turin, Italy
  - 33) Sołtan Institute for Nuclear Studies and Warsaw University, 00-681 Warsaw, Poland<sup>m)</sup>
  - 34) Warsaw University of Technology, Institute of Radioelectronics, 00-665 Warsaw, Poland<sup>n)</sup>
  - 35) Yamagata University, Yamagata, 992-8510 Japan<sup>j)</sup>
  - + ) Deceased
  - a) Also at IST, Universidade Técnica de Lisboa, Lisbon, Portugal
  - b) On leave of absence from JINR Dubna
  - c) Also at Chubu University, Kasugai, Aichi, 487-8501 Japan
  - d) Also at GSI mbH, Planckstr. 1, D-64291 Darmstadt, Germany
  - e) Supported by the German Bundesministerium für Bildung und Forschung
  - f) Supported by Czech Republic MEYS grants ME492 and LA242
  - g) Supported by DST-FIST II grants, Govt. of India
  - h) Supported by the Shailabala Biswas Education Trust
  - i) Supported by the Portuguese FCT - Fundação para a Ciência e Tecnologia grants POCTI/FNU/49501/2002 and POCTI/FNU/50192/2003
  - j) Supported by the Ministry of Education, Culture, Sports, Science and Technology, Japan, Grant-in-Aid for Specially Promoted Research No. 18002006; Daikou Foundation and Yamada Foundation
  - k) Supported by the DFG cluster of excellence ‘Origin and Structure of the Universe’ (www.universe-cluster.de)
  - l) Supported by the Israel Science Foundation, founded by the Israel Academy of Sciences and Humanities
  - m) Supported by Ministry of Science and Higher Education grant 41/N-CERN/2007/0 and the MNII

## 1 Introduction

To fully specify the quark structure of the nucleon at the twist-two level, the transverse spin distributions  $\Delta_T q(x)$  must be added to the better known spin-average distributions  $q(x)$  and to the helicity distributions  $\Delta q(x)$  [1]. Here  $x$  is the Bjorken variable, which represents the momentum fraction of the quarks inside the nucleon. The interpretation of the transversity distribution is similar to that of the helicity distribution, i.e. in a transversely polarised nucleon  $\Delta_T q$  is the difference of the number density of quarks with momentum fraction  $x$  and spin parallel or antiparallel to the nucleon spin. For a discussion on the notation see Refs. [2] and [3].

The distributions  $\Delta_T q$  are difficult to measure, since they are chirally odd and therefore absent in inclusive deep inelastic scattering (DIS). They may instead be extracted from measurements of the single-spin azimuthal asymmetries in cross-sections for semi-inclusive DIS (SIDIS) of leptons off transversely polarised nucleons, in which a hadron is also detected in the final state. In these processes the measurable asymmetry is due to the combined effect of  $\Delta_T q$  and a chirally-odd fragmentation function (FF) which describes the spin-dependent part of the hadronization of a transversely polarised quark. At leading twist, the existence of such a naively  $T$ -odd FF arising from final state interaction effects, was predicted by Collins [4] and is now generally known as the Collins effect. In the fragmentation of transversely polarised quarks it is responsible for a left-right asymmetry which is due to a correlation between the spin of the fragmenting quark and the transverse momentum  $\vec{p}_\perp$  of the produced hadron with respect to the quark direction. The  $\vec{p}_\perp$ -dependent fragmentation function of a transversely polarised quark  $q$  into a spinless hadron  $h$  is thus expected to be of the form

$$D_T^h(z, \vec{p}_\perp) = D_q^h(z, p_\perp) + \Delta_T^0 D_q^h(z, p_\perp) \cdot \sin \varphi, \quad (1)$$

where  $D_q^h$  is the unpolarised FF and the ‘‘Collins function’’  $\Delta_T^0 D_q^h$  is the  $T$ -odd part of the FF, responsible for the left-right asymmetry, and  $z$  is the fraction of available energy carried by the hadron. Here  $\varphi$  is the difference of the azimuthal angles of the hadron transverse momentum and the quark spin, relative to the quark direction. As a result, in SIDIS off transversely polarised nucleons the Collins mechanism is responsible for a modulation in the azimuthal distribution of the produced hadrons given by

$$N(\Phi_C) = N_0(1 + \epsilon_C \cdot \sin \Phi_C). \quad (2)$$

In a gamma–nucleon reference system (GNS), in which the  $z$ -axis coincides with the virtual photon direction and the  $x$ - $z$  plane is the lepton scattering plane, the ‘‘Collins angle’’  $\Phi_C$  is  $\Phi_C = \phi_h + \phi_S - \pi$ . Here  $\phi_h$  is the azimuthal angle of the transverse momentum  $\vec{p}_T^h$  of the outgoing hadron and  $\phi_S$  is the azimuthal angle of the transverse spin vector  $\vec{S}$  of the target nucleon, as shown in Fig. 1. The measurable asymmetry  $\epsilon_C$  is related to the convolution of the transversity parton distribution function (PDF)  $\Delta_T q$  and the Collins function.

An entirely different mechanism was suggested by Sivers [5] as a possible cause of the transverse spin effects observed in  $pp$  scattering. This mechanism could also be responsible for a spin asymmetry in the cross-section of SIDIS of leptons off transversely polarised nucleons. Sivers’ conjecture was based on a possible existence of a correlation

---

research funds for 2005–2007

<sup>n)</sup> Supported by KBN grant nr 134/E-365/SPUB-M/CERN/P-03/DZ299/2000

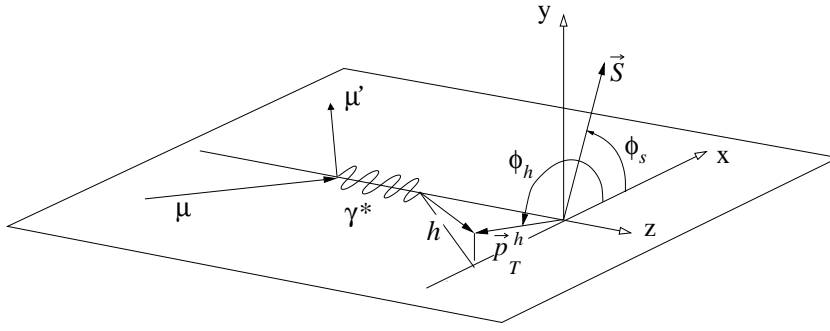


Figure 1: Definition of the azimuthal angle  $\phi_h$  of the transverse momentum  $\vec{p}_T^h$  of the outgoing hadron and of the azimuthal angle  $\phi_s$  of the transverse spin vector  $\vec{S}$  of the target nucleon.

between the intrinsic transverse momentum  $\vec{k}_\perp$  of a quark and the transverse polarisation vector of the nucleon  $\vec{S}$ , i.e. that the quark distribution  $q(x)$  could be written as

$$q_T(x, \vec{k}_\perp) = q(x, k_\perp) + |\vec{S}| \cdot \Delta_0^T q(x, k_\perp) \cdot \sin \varphi', \quad (3)$$

where  $\varphi'$  is the difference of the azimuthal angles of the transverse spin of the nucleon and of the quark transverse momentum, relative to the nucleon direction. In SIDIS off transversely polarised nucleons the Sivers mechanism results in a modulation in the azimuthal distribution of the produced hadrons

$$N(\Phi_S) = N_0(1 + \epsilon_S \cdot \sin \Phi_S), \quad (4)$$

where the ‘‘Sivers angle’’  $\Phi_S = \phi_h - \phi_s$  is the relative azimuthal angle between the transverse momentum of the hadron  $p_T^h$  and the nucleon target spin in the GNS. In this case, the measurable asymmetry  $\epsilon_S$  is related to the convolution of the Sivers PDF  $\Delta_0^T q$  and the unpolarised FF  $D_q^h$ .

Since the Collins and Sivers terms in the transverse spin asymmetry depend on the two independent angles  $\Phi_C$  and  $\Phi_S$ , measuring SIDIS on a transversely polarised target allows the Collins and the Sivers effects to be disentangled, and the two asymmetries can separately be extracted from the data. The same is true for the other azimuthal asymmetries which appear in the general expression of the SIDIS cross-section in the one photon exchange approximation [6]. Correlations between the different terms can be introduced by a non-constant acceptance of the apparatus.

Collins and Sivers modulations have been shown experimentally to be non zero by the HERMES measurements of pion asymmetries in SIDIS on a proton target [7, 8]. Independent information on the Collins function has been provided by the azimuthal correlations in  $e^+e^- \rightarrow$  hadrons measured by the BELLE Collaboration [9]. COMPASS has already published results for the Collins and Sivers asymmetries with a deuteron target for non-identified hadrons [10, 11], and the details of the experimental technique can be found there. Here we present the Collins and Sivers asymmetries on a transversely polarised deuteron target for identified hadrons, i.e. charged pions, and charged and neutral kaons, which put more stringent constraints on a flavour separated analysis of these new transverse spin effects.

## 2 The COMPASS experiment and the SIDIS event selection

The COMPASS experiment is set up at the M2 beam line at CERN, using both muon and hadron beams. For this measurement a longitudinally polarised  $\mu^+$  beam of 160 GeV/ $c$  momentum was scattered off a solid  ${}^6\text{LiD}$  polarised target consisting of two cylindrical cells along the beam direction. The two cells were polarised in opposite directions, so that data were taken simultaneously on oppositely polarised targets to reduce the systematic errors. The target polarisation direction could be set either parallel or orthogonal to the beam direction.

Particle tracking and identification are performed in a two-stage spectrometer, covering a wide kinematical range. A Ring Imaging Cherenkov detector (RICH-1) and two hadron calorimeters provide particle identification. The RICH-1 [12] detector is a gas RICH with a 3 m long  $\text{C}_4\text{F}_{10}$  radiator covering the whole spectrometer acceptance. Two spherical mirror surfaces reflect and focus the Cherenkov photons on two sets of detectors outside the acceptance region. The photon detection utilises multiwire proportional chambers (MWPC) with segmented CsI photocathodes which detect photons in the UV region. The trigger system comprises hodoscope counters and hadron calorimeters. Veto counters installed in front of the target are used to reject the beam halo. A detailed description of the spectrometer can be found in Ref. [13].

The COMPASS Collaboration has taken data with the  ${}^6\text{LiD}$  target polarised transversely with respect to the incoming beam direction in 2002, 2003, and 2004. The transversity data were taken for about 20% of the available beam time. During data taking, particular care was taken to ensure the stability of the apparatus. The target polarisation was typically reversed every 5 days to reduce systematic effects due to the different acceptances of the two cells. To guarantee that the acceptance of the detector fulfills the stability requirements the distributions of several physical quantities ( $x$ ,  $\vec{p}_T^h$ , ...) have been monitored.

In the data analysis, the selection of events required a “primary vertex”, defined by the incoming and the scattered muon tracks, and at least one hadron outgoing from the primary vertex. In addition the projected beam track was required to cross both target cells. Clean hadron and muon selection was achieved using the hadron calorimeters and considering the amount of traversed material. To select DIS events, cuts on the photon virtuality  $Q^2 > 1$  (GeV/ $c$ )<sup>2</sup> and the mass of the hadronic final state  $W > 5$  GeV/ $c^2$  were applied. The requirement of  $0.1 < y < 0.9$ , where  $y$  is the fractional energy of the virtual photon, limits the error due to radiative corrections and avoids contamination from  $\pi$  decay (upper cut), and warrants a good determination of  $y$  (lower cut). To safely reconstruct the hadron azimuthal angle  $\phi_h$  a minimum transverse momentum  $p_T^h$  of 0.1 GeV/ $c$  is required. Furthermore, to select the current fragmentation region, a lower limit for the relative energy of the hadron  $z$  is required. In the following, all hadrons with  $z > 0.2$  define the “all hadron” sample. The analysis is performed also for “leading hadrons” only, for which we expect an enhancement of the physics signal albeit lower statistics. The “leading hadron” is defined as the most energetic hadron coming from the primary vertex and having  $z > 0.25$ . Detailed information on the data analysis can be found in Ref. [11]. Additional cuts specific to the analysis of the identified charged and neutral hadrons are described in the next sections.

## 3 Charged particle identification

Charged hadrons are identified as  $\pi$  and  $K$  using the RICH-1 detector. Several variables have been monitored to ensure the stability in time of the RICH-1 response.

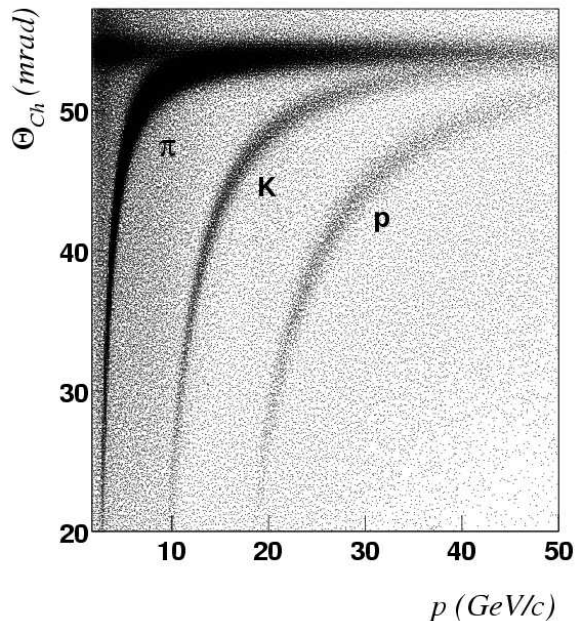


Figure 2: The Cherenkov angle as measured with RICH-1 versus the particle momentum as measured by the spectrometer.

The monitored variables are the hit multiplicities of the MWPCs, the mass hypothesis likelihood (described later in this section), and the number of hadrons identified as  $\pi$  and  $K$  normalised to the number of reconstructed tracks. Blocks of data are rejected if any of the variables deviates from the mean values by more than three standard deviations.

The identification procedure relies on a likelihood function constructed with the photons detected in RICH-1 and associated to the charged particle trajectory. The likelihood function uses the photons of the signal and the theoretical expectation from the Frank and Tamm equation, taking into account possible signal losses due to dead zones in the detector. The description of the background photons, coming from other particles in the event and from the beam halo, is taken from the photon detectors occupancy in the data.

Since the number of Cherenkov photons depends on the velocity of the particle, for a given momentum the signal yield is different for different mass hypotheses. Thus for each track the likelihood is computed for different mass and the background hypotheses. The particle identification is made by choosing the mass hypothesis corresponding to the highest value of the likelihood. To assure a clear distinction from the background, a cut on the ratio of the highest likelihood to the background likelihood is made. To insure a good separation with respect to different masses, a cut on the ratio of the likelihood to the second highest likelihood is also made. The cuts on these variables have been tuned on subsamples of the data considering events in which at least two oppositely charged hadrons from the primary vertex have been found. The cuts for  $K$  identification have been tuned on the  $\phi$  meson peak in the invariant mass distribution of the two charged hadrons, maximising the product of the  $\phi$  signal and the signal-to-background ratio values in the peak. To tune the cuts for pion identification, we used the same approach, but using the  $\rho$  peak in the invariant mass distribution. In addition, all these cuts have been verified on Monte Carlo data.

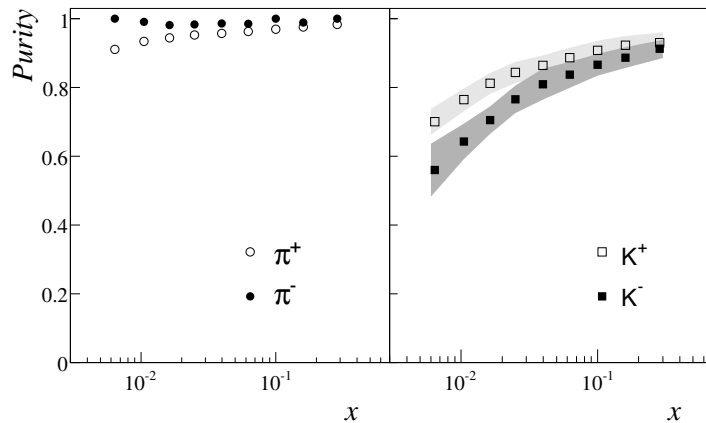


Figure 3: Purities of the pion (left) and kaon (right) samples as a function of  $x$ . The open (closed) points are for positive (negative) pions, while open (closed) squares are for positive (negative) kaons. The shaded area on the right picture gives the evaluated systematic uncertainty for the kaons, while the same is negligible for pions.

In Fig. 2 the dependence of the Cherenkov angle measured by the RICH-1 against the particle momentum clearly indicates the different regions in which hadrons can be identified. In particular, the Cherenkov thresholds are visible: they are about 2.6 GeV/ $c$  for  $\pi$ , 9 GeV/ $c$  for  $K$ , and 17 GeV/ $c$  for protons. To assure a minimum number of detected photons the hadron momenta have to be 0.5 GeV/ $c$  above threshold for pions and 1 GeV/ $c$  above threshold for kaons. The values chosen correspond to 4 emitted photons. The upper limit for the momentum has been set to 50 GeV/ $c$  for both  $\pi$  and  $K$ , corresponding to  $1.5 \sigma$  mass separation between these two mass hypotheses.

The purity of the identified hadrons, defined as the fraction of pions inside the identified pion sample, and the fraction of kaons inside the identified kaon sample, has been evaluated from the data. The results for this analysis are shown in Fig. 3 for positive and negative pions (left) and kaons (right) as a function of  $x$ . While the purity for pions is very high and almost independent from  $x$ , for kaons the purity depends on the momentum and the polar angle of the hadron, and as a consequence it increases with  $x$ . This trend is less pronounced as a function of  $z$  and  $p_T$  given the smaller correlation with the polar angle. On average, purities are higher than 95% for pions, around 70% for negative kaons and around 80% for positive kaons.

The final statistics for the different data taking periods are summarised in Table 1. The use of the RICH-1 information was not possible for the 2002 data, since the functionality of the detector during the transversity run in that year was not satisfactory.

#### 4 $K_S^0$ identification

The reconstruction of the  $K_S^0$  relies on the detection of the two decay pions. The large acceptance of the COMPASS spectrometer provides a good efficiency for the detection of the pion pair. In this part of the analysis the RICH-1 detector is not used to identify the pions.

The signature of  $K_S^0$  events is a  $V_0$  vertex, i.e. a vertex with no incoming but two outgoing charged particles, where the two detected particles have opposite charge. The



Table 1: Final statistics for the “all hadron” and the “leading hadrons” samples.

Year	Period	“all hadrons” ( $\cdot 10^{-6}$ )					“leading hadrons” ( $\cdot 10^{-6}$ )				
		$\pi^+$	$\pi^-$	$K^+$	$K^-$	$K_S^0$	$\pi^+$	$\pi^-$	$K^+$	$K^-$	$K_S^0$
2002	1	-	-	-	-	0.021	-	-	-	-	0.014
2002	2	-	-	-	-	0.014	-	-	-	-	0.009
2003		1.71	1.49	0.31	0.20	0.077	1.10	0.93	0.24	0.14	0.052
2004	1	1.54	1.33	0.27	0.18	0.063	0.98	0.82	0.21	0.13	0.043
2004	2	2.03	1.76	0.36	0.24	0.083	1.30	1.09	0.27	0.17	0.056
Total		5.28	4.58	0.94	0.62	0.258	3.38	2.84	0.72	0.44	0.175

sum of the two outgoing particle momenta must point to the primary vertex and the invariant mass of the two particle system, assuming pion mass for each of them, must agree with the  $K_S^0$  mass. In order to identify  $K_S^0$  from the primary vertex, all  $V_0$  vertices downstream of the primary vertex have been considered. Moreover, the outgoing tracks are not allowed to be additionally associated with any primary vertex and have to satisfy the criteria of section 2. To test the association of the secondary vertex to the primary vertex, the angle between the reconstructed momentum of the hadron pair and the vector connecting the primary and the secondary vertex is calculated. A maximum angle of 10 mrad is accepted. To ensure a proper distinction of the primary and secondary vertices a cut on the distance of the primary and the secondary vertex is chosen on the basis of the signal-to-background ratio for the  $K_S^0$  signal. A distance of about 10 cm yields a good background suppression. Fig. 4 shows the Armenteros plot of the hadron pair, where the transverse momentum  $p_T$  of one of the hadrons relative to the hadron momentum sum is plotted vs. the difference of the longitudinal momenta over their sum  $(p_{L1} - p_{L2})/(p_{L1} + p_{L2})$ . In this plot the  $K_S^0$  band is clearly seen, as well as the  $\Lambda$  and  $\bar{\Lambda}$  bands. To reduce the background due to  $e^+e^-$  pairs a lower cut on  $p_T$  of 25 MeV is applied. To finally identify the  $K_S^0$  candidates a cut on the invariant mass is applied. The reconstructed invariant mass is required to be within  $\pm 20$  MeV of the known mass as shown in Fig. 5. Since the width of the fitted peak is  $\sigma \approx 6$  MeV, the region of  $\pm 20$  MeV covers more than 99 % of the signal. Finally, the kaon transverse momentum with respect to the virtual photon direction is required to be larger than 0.1 GeV/ $c$  to assure a good resolution in the measured azimuthal angle. After all these cuts, the signal-to-background ratio is about 15, constant over all the kinematic range.

Very much as for the charged hadron case, both “leading  $K_S^0$ ” and “all  $K_S^0$ ” samples have been considered. In Table 1 the final statistics used for the asymmetry evaluation is given for all the periods.

## 5 Extraction of the asymmetries

The Collins and Sivers asymmetries for “all” and “leading” pions and kaons have been evaluated separately in kinematical bins of  $x$ ,  $p_T^h$  and  $z$  while the other two variables were integrated over. The number of events  $N_{j,k}^\pm$  in the upstream and downstream target cell ( $k = u, d$ ) for the two polarisations (+, -) in a given  $\Phi_j$  bin ( $j = C, S$  refers to Collins

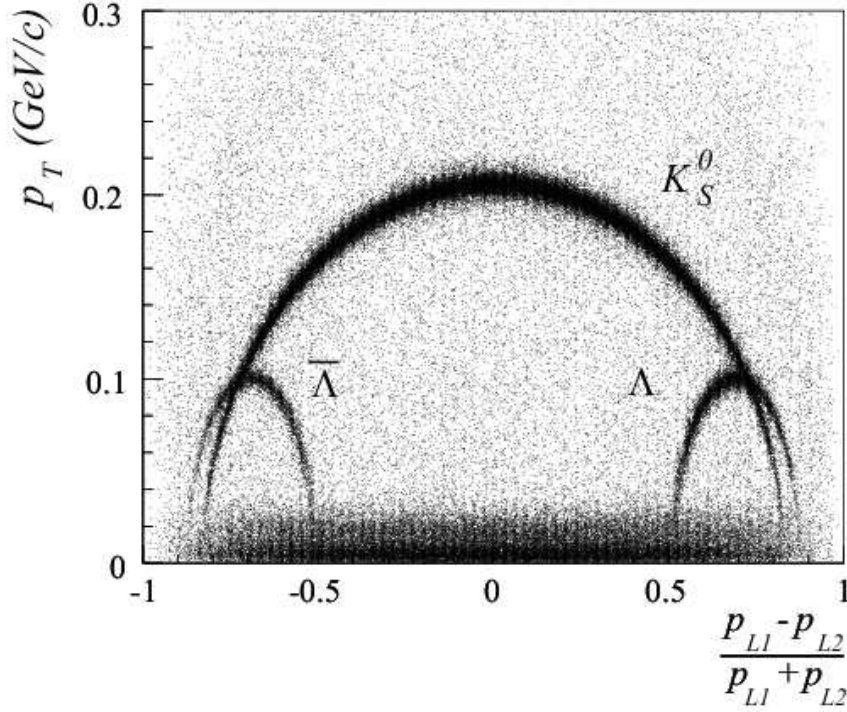


Figure 4: Armenteros plot of the hadron pair. The  $K_S^0$  band can be clearly seen as well as the  $\Lambda$  and  $\bar{\Lambda}$  bands.

and Sivers) can be written as

$$N_{j,k}^{\pm} = F_k^{\pm} n_k \sigma a_{j,k}^{\pm}(\Phi_j) \cdot (1 \pm \epsilon_{j,k}^{\pm} \sin \Phi_j). \quad (5)$$

Here  $F$  is the integrated incident muon flux,  $n$  the number of target particles,  $\sigma$  the spin averaged cross-section and  $a_j$  the product of angular acceptance and efficiency of the spectrometer. The quantities  $\epsilon_{j,k}^{\pm}$  are given by

$$\epsilon_{C,k}^{\pm} = f \cdot P_{T,k}^{\pm} \cdot D_{NN} \cdot A_{Coll}, \quad \epsilon_{S,k}^{\pm} = f \cdot P_{T,k}^{\pm} \cdot A_{Siv}, \quad (6)$$

where  $A_{Coll}$  and  $A_{Siv}$  are the ‘‘Collins’’ and ‘‘Sivers’’ asymmetries, related to the transversity and Sivers PDF respectively. The quantity  $D_{NN} = (1 - y)/(1 - y + y^2/2)$  is the transverse spin transfer coefficient from the target quark to the struck quark,  $f$  is the dilution factor and  $P_{T,k}^{\pm}$  the absolute value of the polarisation of the target cells. The dilution factor has been evaluated taking into account the radiative corrections for hadronic events, and is taken as constant,  $f = 0.38$ , known to 5%. The target polarisation  $P_{T,k}^{\pm}$  has been measured for each cell and for each period [11] and averages to 48% with a relative error of 5%.

From the measured number of events  $N_{j,k}^{\pm}$ , the ratio products

$$A_j(\Phi_j) = \frac{N_{j,u}^+(\Phi_j)}{N_{j,u}^-(\Phi_j)} \cdot \frac{N_{j,d}^+(\Phi_j)}{N_{j,d}^-(\Phi_j)}, \quad j = C, S \quad (7)$$

are computed and fitted with the functions  $p_0 \cdot (1 + \hat{A}_j \cdot \sin \Phi_j)$  to extract the raw Collins and Sivers asymmetries. Due to the smallness of the asymmetries involved,  $\hat{A}_j$  is to a good approximation  $\hat{A}_j = \epsilon_{j,u}^+ + \epsilon_{j,d}^+ + \epsilon_{j,u}^- + \epsilon_{j,d}^-$ . The fit is performed in the interval  $(0, 2\pi)$  which

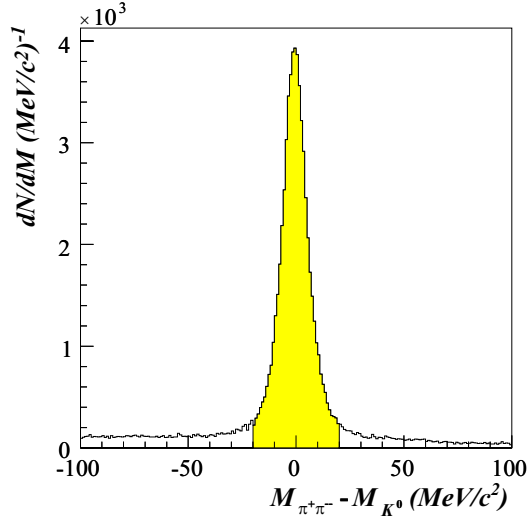


Figure 5: Difference of the invariant mass of the hadron pair after cuts to the  $K_S^0$  mass. The shaded region shows the accepted  $K_S^0$ .

is divided into 16 bins for charged hadrons and 8 bins for  $K_S^0$  due to the low statistics. From Monte Carlo simulations it is found that the angular resolution is much better than the bin size.

The Collins and Sivers asymmetries have been evaluated separately in each kinematic bin and for each data taking period; the results for the different periods have been combined using the weighted mean. Finally using the purities a purity matrix  $P$  can be written

$$P = \begin{pmatrix} P_{\pi,\pi} & P_{K,\pi} \\ P_{\pi,K} & P_{K,K} \end{pmatrix}, \quad (8)$$

here  $P_{\pi,\pi}$  ( $P_{K,K}$ ) is the fraction of real pions (kaons) inside the identified pion (kaon) sample and  $P_{\pi,K}$  ( $P_{K,\pi}$ ) is the fraction of misidentified kaons (pions) inside the pion (kaon) sample. Due to the fact that the contribution of other particles (like protons) was found to be negligible it is assumed that  $P_{\pi,K} = 1 - P_{\pi,\pi}$  and  $P_{K,\pi} = 1 - P_{K,K}$ . The relation between measured  $A^m$  and corrected  $A^c$  asymmetries is

$$\vec{A}^c = P^{-1} \vec{A}^m \quad \text{with} \quad \vec{A} = \begin{pmatrix} A_\pi \\ A_K \end{pmatrix}. \quad (9)$$

This gives for the kaons

$$A_K^c = \frac{1}{P_{\pi,\pi} + P_{K,K} - 1} \left[ P_{\pi,\pi} A_K^m - (1 - P_{K,K}) A_\pi^m \right]. \quad (10)$$

This equation contains two terms; the first accounts for the dilution of the kaon asymmetry due to the purity of the sample, the second removes the contribution of the pion asymmetry from the identified kaons. Since both pion and kaon asymmetries on the deuteron target are compatible with zero over the full range, this second term has been put to zero,

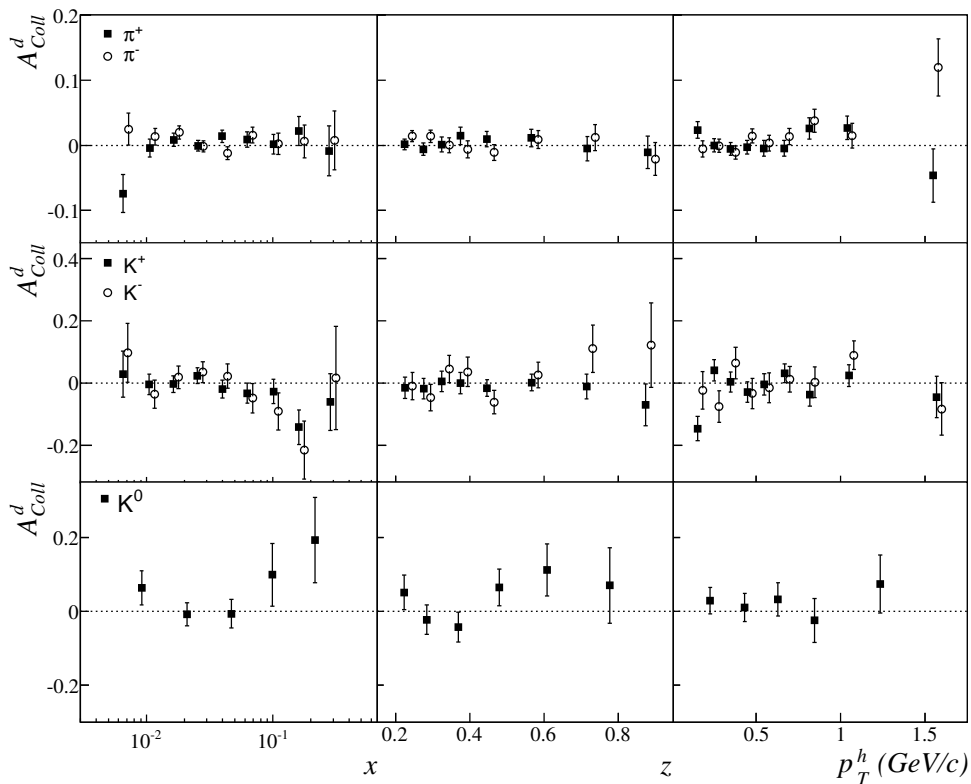


Figure 6: Collins asymmetry against  $x$ ,  $z$  and  $p_T^h$  for the “all” charged pions and kaons samples from the 2003–2004 data, and the “all”  $K_S^0$ ’s sample from the 2002–2004 data.

both in Eq. (10) and in the equation giving  $A_\pi^c$ , and the errors have been evaluated correspondingly.

The same approach was followed for the neutral kaons, where it has been checked that the asymmetry of the background under the  $K_S^0$  peak was compatible with zero.

## 6 Results and conclusion

The final results for the Collins and Sivers asymmetries  $A_{Coll}$  and  $A_{Siv}$  for charged pions and charged and neutral kaons on the deuteron target vs. the three kinematic variables  $x$ ,  $z$  and  $p_T^h$  are given in Figs. 6–9.<sup>1)</sup> In the figures, the data points for negative hadrons, which are calculated in the same  $x$ -,  $z$ - and  $p_T$ -bin as for the positive hadrons, have been slightly shifted for graphical reasons.

Extensive studies to evaluate the size of the systematic error have been performed. For some of these studies the  $z$  cut has been opened and the data sample has been enlarged by a factor of three. The measured Collins and Sivers asymmetries were checked against stability among the five different periods of data taking, against the use of different estimators to extract the asymmetries, against the reduction of the fiducial volume of our spectrometer and against the influence of the trigger system of the experiment. In these studies no deviations from the real asymmetries beyond the expected statistical fluctuations was observed. Furthermore experimental false asymmetries have been studied by combining the data set in such a way that the extracted asymmetries are expected to be zero. During all these tests no asymmetries deviating from zero with statistical

<sup>1)</sup> All the numerical values, including the purities, are available on HEPDATA.

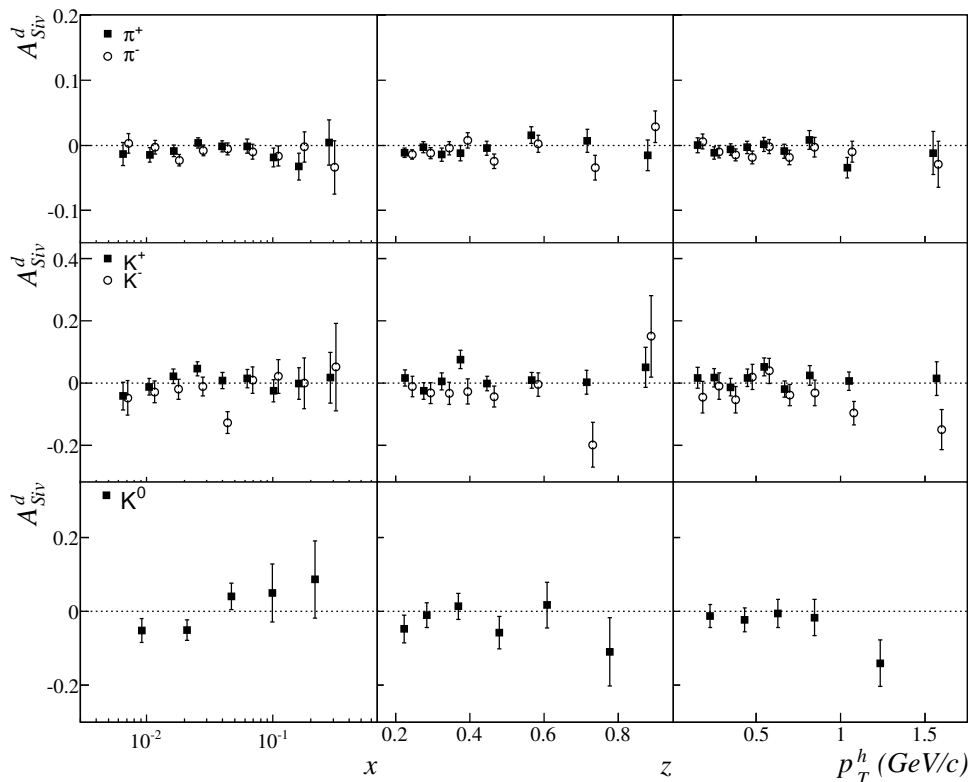


Figure 7: Sivers asymmetry against  $x$ ,  $z$  and  $p_T^h$  for the “all” charged pions and kaons samples from the 2003–2004 data, and “all”  $K_S^0$ ’s sample from the 2002–2004 data.

significance was observed.

Also, the correlation between the measured Collins and Sivers asymmetries which originates from the non-uniform  $\phi_h/\phi_S$  acceptance of the spectrometer has been studied and the corresponding systematic error has been evaluated to be negligible as compared with the statistical error. The smallness of the asymmetries makes the systematic error due to the uncertainties on  $P_T$  and  $f$  totally negligible. These studies altogether lead to the final conclusion that the systematic errors are considerably smaller (well below 30%) than the statistical errors.

All the measured asymmetries are small, a trend which was already observed in the published data of the non-identified hadrons. Small asymmetries are not a surprise, it was expected that transverse spin effects be small in the deuteron due to the opposite sign which was predicted for the u- and d-quark distributions, very much like in the helicity case.

The interpretation of the results on the deuteron can be done only in conjunction with corresponding proton data, measured by the HERMES Collaboration albeit at lower energy. Proton target data have been collected by COMPASS in 2007, but the results are not final at the time of writing. As shown in Refs. [8, 11] a simple analysis of the HERMES charged pion data and of the non-identified charged hadron data in COMPASS, assuming that all the hadrons are pions, led to the following conclusions:

1. the favoured and unfavoured Collins functions have about the same size and the COMPASS deuteron data are needed for the extraction of the d-quark transversity;
2. the null result for the Sivers asymmetry for the COMPASS data is a clear indication

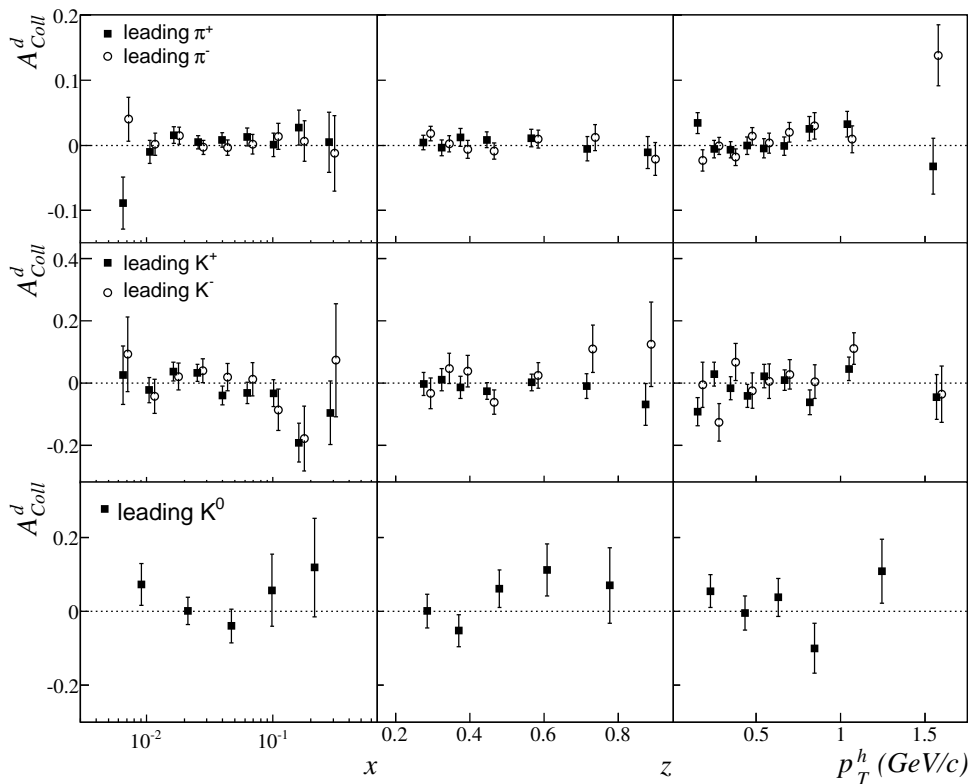


Figure 8: Collins asymmetry against  $x$ ,  $z$  and  $p_T^h$  for the “leading” charged pions and kaons samples from the 2003–2004 data, and “leading”  $K_S^0$ ’s sample from the 2002–2004 data.

that the u- and d-quark Siverson distribution functions have about the same size and opposite sign.

The same conclusions have been obtained in several analyses, using more sophisticated tools (see e.g. Refs. [14–16]). A first global analysis which combined the 2002–2004 HERMES pion Collins asymmetries, the COMPASS results for non-identified hadrons, and the BELLE data has recently allowed to extract the Collins functions and, for the first time, the transversity distributions for the u- and d-quark [17]. Similar analyses can be now done including the present pion data which put more stringent constraints.

The kaon data again show small asymmetries. In the case of the charged kaons, although the statistics is a factor of about 6 smaller than for the pions, the error bars are still rather small. The neutral kaon sample is smaller in size by a factor of about 3 with respect to the charged kaons, and the error bars start being large. The COMPASS data do not exhibit the large difference between  $K^+$  and  $\pi^+$  asymmetries seen by HERMES. Very much like for the  $\pi^\pm$  case, cancellations are expected between u- and d-quarks when using the isoscalar deuteron target. Therefore the smallness of the COMPASS kaon asymmetries suggests that the sea quark contributions to the asymmetries are small. The kaon data provide a unique handle on the s-quark, but in this case the sea-quark contributions can not be neglected, and a full global analysis including pions and kaons is mandatory.

To summarise, COMPASS has made the first precise measurements of the Collins and Siverson asymmetries for charged pions with a transversely polarised deuteron target. The same asymmetries have also been obtained for charged and neutral kaons. All the

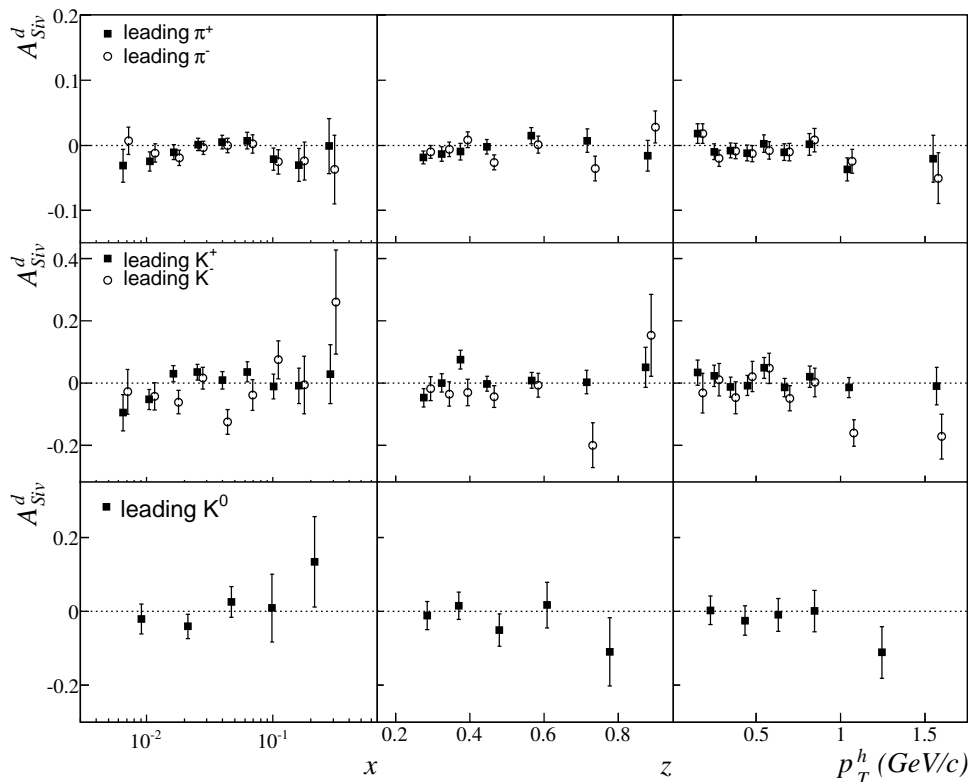


Figure 9: Siivers asymmetry against  $x$ ,  $z$  and  $p_T^h$  for the “leading” charged pions and kaons samples from the 2003–2004 data, and “leading”  $K_S^0$ ’s sample from the 2002–2004 data.

measured asymmetries are small, pointing at a cancellation between the u- and d-quarks contributions. More quantitative information, in particular for the s-quark distributions, can be obtained with global analyses, in which the COMPASS measurements with a transversely polarised proton target undoubtedly will play an important role.

We acknowledge the support of the CERN management and staff, the special support of CEA/Saclay in the target magnet project, as well as the skills and efforts of the technicians of the collaborating institutes.

## References

- [1] R. L. Jaffe and X. D. Ji, Phys. Rev. Lett. **67** (1991) 552.
- [2] V. Barone, A. Drago and P. G. Ratcliffe, Phys. Rept. **359** (2002) 1.
- [3] A. Bacchetta *et al.*, Phys. Rev. D **70** (2004) 117504.
- [4] J. C. Collins, Nucl. Phys. B **396** (1993) 161.
- [5] D. W. Sivers, Phys. Rev. D **41** (1990) 83.
- [6] A. Bacchetta *et al.*, JHEP **0702** (2007) 093 and references therein.
- [7] A. Airapetian *et al.* [HERMES Collaboration], Phys. Rev. Lett. **94** (2005) 012002.
- [8] M. Dieffenthaler [HERMES Collaboration], arXiv:0706.2242 [hep-ex].
- [9] K. Abe *et al.* [Belle Collaboration], Phys. Rev. Lett. **96** (2006) 232002.
- [10] V. Y. Alexakhin *et al.* [COMPASS Collaboration], Phys. Rev. Lett. **94** (2005) 202002.
- [11] E. S. Ageev *et al.* [COMPASS Collaboration], Nucl. Phys. B **765** (2007) 31.
- [12] E. Albrecht *et al.*, Nucl. Instr. and Meth. A **553** (2005) 215 and references therein.

- [13] P. Abbon *et al.* [COMPASS Collaboration], Nucl. Instrum. Meth. A **577** (2007) 455.
- [14] M. Anselmino, M. Boglione, U. D'Alesio, A. Kotzinian, F. Murgia and A. Prokudin, Phys. Rev. D **72** (2005) 094007, [Erratum, *ibid.* D **72** (2005) 099903].
- [15] W. Vogelsang and F. Yuan, Phys. Rev. D **72** (2005) 054028.
- [16] A. V. Efremov, K. Goeke and P. Schweitzer, Czech. J. Phys. **56** (2006) F181.  
A. V. Efremov, K. Goeke and P. Schweitzer, Phys. Rev. D **73** (2006) 094025.
- [17] M. Anselmino *et al.*, Phys. Rev. D **75** (2007) 054032.